Hydroxyl Radical Generation by Photosystem II[†]

Pavel Pospíšil,*[,‡] András Arató,[§] Anja Krieger-Liszkay,[§] and A. William Rutherford[‡]

Service Bioénérgetique, Département de Biologie Joliot Curie, CEA Saclay, F-91191 Gif-sur-Yvette, France, and Institut für Biologie II, Biochemie der Planzen, Universität Freiburg, Schänzlestrasse 1, 79104 Freiburg, Germany

Received December 10, 2003; Revised Manuscript Received March 26, 2004

ABSTRACT: The photogeneration of hydroxyl radicals ($OH^•$) in photosystem II (PSII) membranes was studied using EPR spin-trapping spectroscopy. Two kinetically distinguishable phases in the formation of the spin trap-hydroxyl (POBN-OH) adduct EPR signal were observed: the first phase ($t_{1/2} = 7.5$ min) and the second phase ($t_{1/2} = 30$ min). The generation of $OH^•$ was found to be suppressed in the absence of the Mn-complex, but it was restored after readdition of an artificial electron donor (DPC). Hydroxyl radical generation was also lost in the absence of oxygen, whereas it was stimulated when the oxygen concentration was increased. The production of $OH^•$ during the first kinetic phase was sensitive to the presence of SOD, whereas catalase and EDTA diminished the production of $OH^•$ during the second kinetic phase. The POBN-OH adduct EPR signal during the first phase exhibits a similar pH-dependence as the ability to oxidize the non-heme iron, as monitored by the Fe^{3+} ($g = 8$) EPR signal: both EPR signals gradually decreased as the pH value was lowered below pH 6.5 and were absent at pH 5. Sodium formate decreases the production of $OH^•$ in intact and Mn-deleted PSII membranes. Upon illumination of PSII membranes, both superoxide, as measured by EPR signal from the spin trap-superoxide (EMPO-OOH) adduct, and H_2O_2, measured colormetrically, were generated. These results indicated that $OH^•$ is produced on the electron acceptor side of PSII by two different routes, (1) $O_2^{•-}$, which is generated by oxygen reduction on the acceptor side of PSII, interacts with a PSII metal center, probably the non-heme iron, to form an iron-peroxide species that is further reduced to $OH^•$ by an electron from PSII, presumably via Q_A^-, and (2) $O_2^{•-}$ dismutates to form free H_2O_2 that is then reduced to $OH^•$ via the Fenton reaction in the presence of metal ions, the most likely being Mn^{2+} and Fe^{2+} released from photodamaged PSII. The two different routes of $OH^•$ generation are discussed in the context of photoinhibition.

Photosystem II (PSII)[1], a pigment−protein complex embedded in the thylakoid membrane of higher plants, algae, and cyanobacteria, catalyzes the light-driven oxidation of water and reduction of plastoquinone (*1*−*5*). As a byproduct of the photosynthetic oxidation of water, molecular oxygen is evolved. Molecular oxygen acts in two different ways in the photosynthetic processes: (1) O_2 is used as a sink for electrons (e.g., in the absence of CO_2) (*6*), and (2) O_2 is a source of reactive oxygen species (ROS), which are known to attack proteins, lipids, or nucleic acids (*7*, *8*). Oxygen is reduced in successive univalent reactions to form superoxide radical ($O_2^{•-}$), hydrogen peroxide (H_2O_2), and hydroxyl radical ($OH^•$) (Scheme 1A). While $O_2^{•-}$ and H_2O_2 are relatively unreactive, $OH^•$ is highly reactive and therefore potentially dangerous for PSII components (*9*).

The light-induced formation of $O_2^{•-}$ produced by PSII was demonstrated either indirectly by an assay involving cytochrome *c* reduction in the presence of xanthine/xanthine oxidase (*10*) or directly by voltametric methods (*11*). EPR evidence for the production of $O_2^{•-}$ in PSII membranes was provided by using the spin trap compound DEPMPO (*12*, *13*). It was proposed that $O_2^{•-}$ is formed by the reduction of molecular oxygen on the electron acceptor side of PSII, and either $Pheo^-$ or Q_A^- were suggested to be the reductant for O_2 (*10*, *11*). Superoxide was also proposed to be formed by the one-electron oxidation of H_2O_2 by a strong oxidant on the electron donor side of PSII (*14*, *15*).

Whereas the production of $O_2^{•-}$ is rather uncontroversial, the site and mechanism by which H_2O_2 is produced are a matter of debate. H_2O_2 was shown to be produced in PSII depleted of the 17, 23, and/or 33 kDa extrinsic proteins (*16*−*18*) and also Cl^--depleted PSII (*19*−*21*). The production of H_2O_2 was suggested to originate from the dismutation of $O_2^{•-}$ generated on the PSII electron acceptor side (*22*, *17)*. The cyt b_{559} or the non-heme iron were suggested as the most feasible candidates for SOD activity in PSII (*10*, *12*, *23*, *24*). On the other hand, several authors suggested that H_2O_2 was produced on the PSII donor side (*17*−*19*, *21*, *25*). A short-

[†] This work was supported by the Marie Curie individual fellowship (HPMF-CT-2001−01123).

* Correspondence should be addressed to Dr. Pavel Pospíšil, Service Bioénergétique, Département de Biologie Joliot Curie, CEA Saclay, F-91191 Gif-sur-Yvette, France. Telephone: +33.01.69.08.86.57. Fax: +33.01.69.08.87.17. E-mail: pospisil@dsvidf.cea.fr.

[‡] CEA Saclay.

[§] Universität Freiburg.

[1] Abbreviations: Cyt b_{559}, cytochrome b_{559}; DPC, diphenylcarbazide; DCPIP, 2,6-dichlorophenolindophenol; DEPMPO, 5-diethoxyphosphoryl-5-methyl-1-pyrroline-*N*-oxide; DMPO, 5,5-dimethyl-1-pyrroline-*N*-oxide; EDTA, ethylenediaminetetraacetic acid; EMPO, 5-(ethoxycarbonyl)-5-methyl-1-pyrroline *N*-oxide; EPR, electron paramagnetic spectroscopy; Mes, 2-(*N*-morpholino) ethanesulfonic acid; NH_2OH, hydroxylamine; PSII, photosystem II; Pheo, pheophytin − primary electron acceptor of PSII; POBN, 4-pyridyl-1-oxide-*N*-*tert*-butylnitrone; P680, primary electron donor of PSII; Q_A, primary plastoquinone electron acceptor of PSII; SOD, superoxide dismutase; SOR, superoxide reductase; DTPA, diethylenetriamine penta-acetic acid.

10.1021/bi036219i CCC: $27.50
Published on Web 05/06/2004

Scheme 1[a]

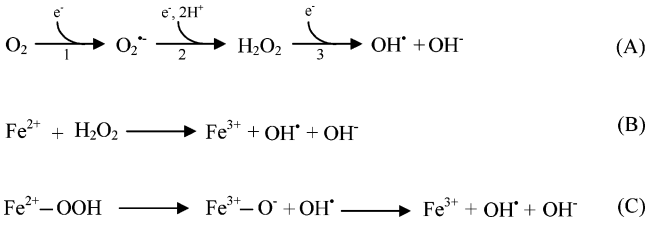

[a] (A) Successive univalent reduction of molecular oxygen to OH•. The reaction pathway involves (1) one-electron reduction of molecular oxygen to $O_2^{\bullet-}$, (2) dismutation of $O_2^{\bullet-}$ to H_2O_2, and (3) one-electron reduction of H_2O_2 to OH•. (B) Iron-driven reduction of H_2O_2 to OH• via Fenton reaction. (C) Iron-driven reduction of bound peroxide to OH• via iron-oxo intermediate.

circuiting of the S-state cycle (*19*) or nucleophilic attack of a hydroxo ligand by a terminal oxo group of the Mn-complex (*26*) were proposed as potential mechanisms for H_2O_2 production on the PSII donor side.

In addition to $O_2^{\bullet-}$ and H_2O_2, illumination of PSII membranes was shown to result in the formation of OH• (*27*). The authors demonstrated by using the DMPO spin trap that production of OH• is enhanced in the presence of copper and suppressed in the absence of oxygen. Navari-Izzo et al. (*12*) showed by using the DEPMPO spin trap that production of OH• is accompanied by the generation of $O_2^{\bullet-}$. Other authors suggested that in addition to the catalase-mediated disproportionation of H_2O_2, free metal ions or the non-heme iron in PSII cause disproportionation of H_2O_2 probably by its reduction to OH• (*28*). The production of both $O_2^{\bullet-}$ and OH• has been recently demonstrated in the presence of either pheonolic or urea-type herbicides (*29*). The authors demonstrated by using the EMPO spin trap, which can be used to trap both $O_2^{\bullet-}$ and OH•, that in the presence of DCMU the production of $O_2^{\bullet-}$ is eliminated by SOD, whereas the production of OH• is diminished by catalase. Using the DMPO spin trap, Hideg et al. (*30*) showed that in Mn-depleted thylakoid membranes OH• is produced by an oxidizing reaction on the PSII donor side. The production of OH• has also been recently demonstrated in the isolated light-harvesting proteins (LHCII) (*31*). This seems to be a singlet oxygen mediated phenomenon associated with the detergent-isolated complexes and so is probably unrelated to the effects seen in the present work.

For a long time, the production of OH• in biological systems was believed to occur by the Fenton reaction, well-known in inorganic chemistry, i.e., the reduction of free H_2O_2 mediated by free metal ions such as Fe^{2+}, Mn^{2+}, or Cu^{+} (Scheme 1B) (*7*, *8*, *32*, *33*). Several lines of evidence have been given supporting the suggestion that in addition to free H_2O_2, OH• might be produced by the reduction of peroxide bound to a metal center (Scheme 1C) (*33*−*38*). Whereas the Fenton reaction involves outer-sphere electron transfer with no direct binding of peroxide to iron, the reduction of bound peroxide proceeds as an inner-sphere electron transfer process that strictly requires direct binding of peroxide to iron. Several iron-peroxide complexes have been proposed to be intermediates in the enzymatic reaction pathway of cytochrome P450 (*39*), bleomycin (*40*), heme oxygenase (*41*), or superoxide reductase (*42*−*44*).

In the present study, EPR spin-trapping spectroscopy was used to investigate light-induced OH• production in PSII membranes. Evidence is given that indicates that OH• is produced by two reaction pathways: (1) the reduction of peroxide bound to PSII metal center (probably the non-heme iron, although the cytochrome b559 heme is not ruled out), and (2) the reduction of free H_2O_2 mediated by free metal ions, the most likely being Mn^{2+} and Fe^{2+} (i.e., via the Fenton reaction).

MATERIALS AND METHODS

Sample Preparation. PSII membranes from spinach were prepared using the method of Berthold et al. (*45*) with the modifications described in Ford and Evans (*46*) and stored at −80 °C until use in 0.4 M sucrose, 15 mM NaCl, 5 mM $MgCl_2$, and 40 mM Mes (pH 6.5). Mn-depleted PSII membranes were prepared by incubation of PSII membranes in a buffer containing 5 mM NH_2OH, 0.4 M sucrose, 15 mM NaCl, 5 mM $MgCl_2$ and 40 mM Mes (pH 6.5) for 1 h at 4 °C. After treatment, PSII membranes were washed twice in the same buffer without NH_2OH.

Photoinhibitory Treatment. Photoinhibition was performed by illuminating the PSII membranes (150 μg of Chl mL^{-1}) in a glass tube with a diameter of 1.5 cm at 20 °C with a continuous white light, intensity 3000 μmol m^{-2} s^{-1}. A water filter and Calflex IR filter were used for heat protection, and the samples were stirred during the treatment. At given time points, the oxygen evolution activity and H_2O_2 were measured.

Measurements of Light-Induced Production of O_2 and H_2O_2. Photosynthetic oxygen evolution was measured in PSII membranes (30 μg of Chl mL^{-1}) with a Clark-type electrode (Hansatech) using 1 mM *p*-phenylbenzoquinone as an electron acceptor. Production of H_2O_2 was measured in PSII membranes (5 μg of Chl mL^{-1}) by oxidation of 1 mM thiobenzamide with 0.1 mM lactoperoxidase (*22*). Thiobenzamide sulfoxide was quantified by its absorbance at 370 nm (extinction coefficient 2.92 10^3 M^{-1} cm^{-1}).

Room-Temperature Spin-Trapping EPR Measurements. The spin-trapping was accomplished by either POBN, 4-pyridyl-1-oxide-*N*-*tert*-butylnitrone (Sigma-Aldrich) or EMPO, 5-(ethoxycarbonyl)-5-methyl-1-pyrroline *N*-oxide (Alexis Biochemicals). PSII membranes (150 μg of Chl mL^{-1}) in glass capillary tubes (internal diameter of 1 mm) were put into quartz EPR tubes (internal diameter of 3 mm) and illuminated directly in the cavity of the EPR spectrometer with continuous white light (3000 μmol m^{-2} s^{-1} at the cavity window, light was filtered through 4 cm of water and Calflex IR filter). For detection of OH•, illumination was done in the presence of 10 mM POBN, 170 mM ethanol, and 25 mM Mes (pH 6.5). For detection of $O_2^{\bullet-}$, 25 mM EMPO, 100 μM DTPA, and 25 mM Mes (pH 6.5) was used. At a given time, the light was turned off and the appropriate spin trap-radical adduct EPR spectrum was collected. For measurements of the time dependence of the POBN-OH adduct EPR signal, the center-field line of the POBN-OH adduct EPR spectrum (indicated by the arrow in Figure 1A) was measured as a function of time during sample illumination. In some measurements, bovine liver catalase (EC 1.11.1.6) (5000 units mL^{-1}), horseradish SOD (EC 1.15.1.1) (400 units mL^{-1}), 1 mM DPC, 1 mM NH_2OH, 30 μM DCPIP, and 1

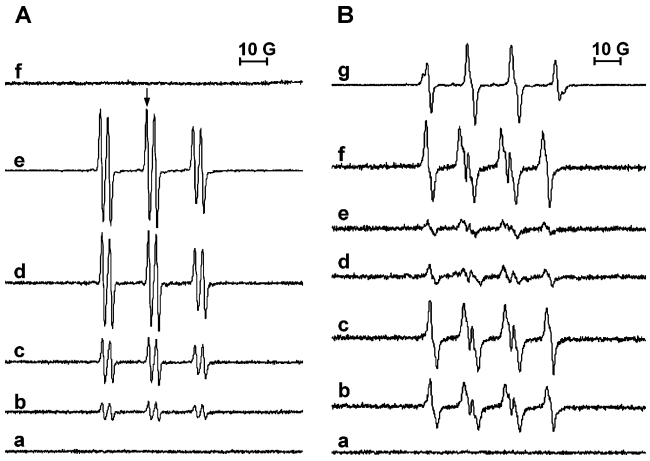

FIGURE 1: (A) Light-induced POBN-OH adduct EPR spectra measured in PSII membranes after illumination for (a) 0, (b) 5, (c) 15, and (d) 45 min. The spectra were recorded in the presence of 10 mM POBN, 170 mM ethanol, 150 μg of Chl mL^{-1} and 25 mM MES (pH 6.5). The spectrum (e) was obtained by addition of 100 μM Fe_2SO_4 to 50 μM H_2O_2 in the presence of 10 mM POBN and 170 mM ethanol. The spectrum (f) was generated by incubation of mixtures contained 1 mM xanthine and 0.05 U mL^{-1} xanthine oxidase in the presence of 10 mM POBN and 170 mM ethanol. (B) Light-induced EMPO-OOH adduct EPR spectra measured in PSII membranes after illumination for (a) 0, (b) 5, (c) 15, (d) 30, and (e) 45 min. The spectra were recorded in the presence of 25 mM EMPO, 100 μM DTPA, 150 μg of Chl mL^{-1} and 25 mM MES (pH 6.5). In traces b and c, EMPO was present during the whole period of illumination. In traces d and e, PSII membranes were first preilluminated in the absence of EMPO for 25 and 40 min, respectively, and then illuminated for 5 min in the presence of EMPO to complete the illumination period. The spectrum (f) was generated by incubation of mixtures contained 1 mM xanthine and 0.05 U mL^{-1} xanthine oxidase in the presence of 100 μM DTPA and 25 mM EMPO. The spectrum (g) was obtained by addition of 100 μM Fe_2SO_4 to 50 μM H_2O_2 in the presence of 25 mM EMPO. In both (A) and (B), the sample was illuminated directly in the EPR cavity with continuous white light of 3.000 μmol m^{-2} s^{-1} prior to the measurements. EPR conditions: microwave power, 1 mW (A) and 3 mW (B); modulation amplitude, 1 G; modulation frequency, 100 kHz; conversion time, 81.92 ms; and time constant, 1.280 ms.

mM EDTA were added before illumination, as indicated in the text.

Low-Temperature EPR Measurements. PSII membranes (5 mg of Chl mL^{-1}) were illuminated in calibrated quartz EPR tubes in the EPR cavity under the same conditions as the sample for the spin-trapping EPR measurements. After illumination, the sample was dark-adapted for 10 min on ice and then subjected to further treatment to generate the appropriate EPR signals. For measurements of the $Q_A^-Fe^{2+}$ EPR signal, the sample was illuminated at 200 K for 10 min in the presence of 100 mM sodium formate (*47*, *48*). For measurements of the Fe^{3+} signal, PSII membranes were incubated in the presence of 5 mM potassium ferricyanide for 30 min on ice in the dark (*49*).

EPR Spectrometer. EPR spectra were recorded with a X-band EPR spectrometer (9.1 GHz, Bruker ESP 300, Karlsruhe, Germany) equipped with an Oxford cryostat and temperature controller (Oxford/UK). The microwave frequency and magnetic field were measured with a microwave frequency counter HP 5350B and a Bruker ER035M NMR gaussmeter, respectively. The data acquisition and data handling were performed with the ESP300 software. The EPR settings were as indicated in the figure legend.

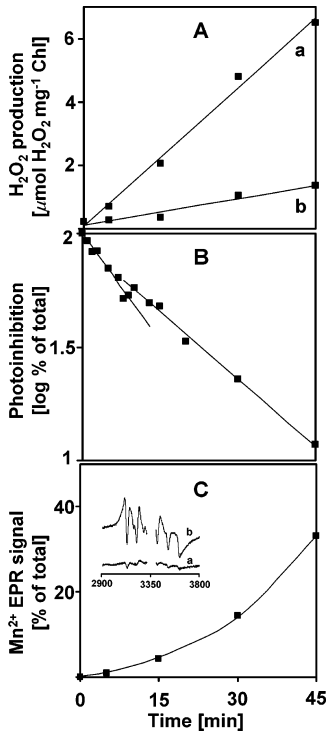

FIGURE 2: (A) Light-induced production of H_2O_2 in PSII membranes measured (a) in the presence and (b) in the absence of O_2. PSII membranes were illuminated in the presence of 1 mM thiobenzamide with 0.1 mM lactoperoxidase under the same conditions as in Figure 1. In (b) O_2 was removed by bubbling of the sample with a gentle stream of argon for 30 s. (B) Photoinhibition of PSII membranes measured as oxygen evolution activity in the presence of 1 mM *p*-phenylbenzoquinone. In the control PSII membranes the oxygen evolving activity was 668 μmol of O_2 (mg of Chl)$^{-1}$ h^{-1}. To clearly see a biphasic loss of oxygen evolution a logarithmic scale is used. (C) Release of manganese from PSII membranes measured by six-line hexaquo-Mn^{2+} EPR signal. The height of signal was calculated as the sum of the amplitudes of three low-field lines. Total concentration of Mn^{2+} was determined in the presence of 0.5 M HCl (*55*). Inset shows six-line hexaquo-Mn^{2+} EPR signal measured after illumination for (a) 0 and (b) 45 min. EPR conditions: temperature, 20 K; microwave power, 32 mW; modulation amplitude, 22 G; modulation frequency, 100 kHz.

RESULTS

OH• Production in PSII. The light-induced production of OH• in PSII membranes was measured using EPR spin-trapping spectroscopy. The spin-trapping was accomplished in the presence of the spin trap compound POBN, which reacts with OH• to form the POBN-OH adduct. No EPR signal was observed in nonilluminated PSII membranes (Figure 1A, trace a), whereas illumination with continuous white light results in the generation of the POBN-OH adduct EPR signal (Figure 1A, traces b−d). The six-line spectra show all the characteristics of the POBN-OH adduct EPR spectra as reported in the literature (*50*, *51*). Figure 1A (trace e) shows POBN-OH adduct EPR spectrum formed by addition of Fe_2SO_4 to H_2O_2. The gradual increase in the POBN-OH adduct EPR signal with illumination time indicates that exposure of PSII membranes to light results in the gradual production of OH•.

To monitor the real-time production of OH• under illumination, the time dependence of light-induced formation of the POBN-OH adduct EPR signal was measured. As is evident from Figure 3A (trace a), the POBN-OH adduct EPR

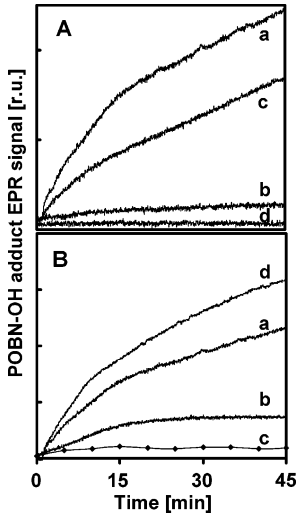

FIGURE 3: (A) Time dependence of the POBN-OH adduct EPR signal measured in (a) active PSII membranes, (b) Mn-depleted PSII membranes, (c) Mn-depleted PSII membranes in the presence of DPC, and (d) Mn-depleted PSII membranes in the presence of DPC and DCPIP. (B) Time dependence of the POBN-OH adduct EPR signal in PSII membranes measured (a) in air, (b) after removal of O_2 before illumination, (c) removal of O_2 during illumination, and (d) at enhanced O_2 concentration. To remove O_2, the sample was bubbled with a gentle stream of argon (b) before the illumination for 30 s and (c) during illumination. The enhanced O_2 concentration was maintained by bubbling of the sample with oxygen for 30 s prior to the illumination. EPR conditions: conversion time, 2.62 s; time constant, 0.327 s; other conditions as in Figure 1.

signal increases in two phases: the first phase ($t_{1/2} = 7.5$ min) and the second phase ($t_{1/2} = 30$ min).

$O_2^{\bullet-}$ Production in PSII. A recently developed spin trap compound EMPO (*52*, *53*) was used to monitor the production of $O_2^{\bullet-}$ in PSII membranes (*21*). No EPR signal was observed in nonilluminated PSII membranes showing that no $O_2^{\bullet-}$ is produced in the dark (Figure 1B, trace a). After illumination of PSII membranes, a spectrum was detected that exhibits the peaks and hyperfine splitting characteristics of spin trap−superoxide adduct (EMPO-OOH) (Figure 1B, traces b−e). A characteristic EMPO-OOH adduct EPR spectrum formed by incubation of xanthine with xanthine oxidase is shown in Figure 1B (trace f). Because of instability of the EMPO-OOH adduct (the lifetime ∼ 15 min) (*53*), illumination of PSII membranes for a longer period results in a decrease in the EMPO-OOH adduct EPR signal (data not shown). To prevent this, PSII membranes were first preilluminated in the absence of EMPO and then illuminated for additional 5 min in the presence of EMPO (Figure 1B, traces d−e). These observations indicate that the illumination of PSII membranes results in the generation of $O_2^{\bullet-}$.

H_2O_2 Production, O_2 Evolution, and Manganese Release. The production of H_2O_2 was measured by oxidation of thiobenzamide with lactoperoxidase (*22*). As is evident from Figure 2A, illumination of PSII membranes in the presence of oxygen results in the production of H_2O_2 (Figure 2A, trace a), whereas removal of oxygen by flushing of the PSII membranes with argon greatly reduced H_2O_2 production (Figure 2A, trace b).

Figure 2B shows the effect of illumination on oxygen evolving activity. The oxygen evolving activity was gradually lost during the time-course of illumination. The loss of oxygen evolving activity was biphasic—during the first phase of illumination ($t_{1/2} = 7.5$ min) the loss of activity was faster than during the second phase ($t_{1/2} = 30$ min). A similar time-course of photoinhibition was also reported previously (*54*).

To investigate whether illumination led to a loss of manganese, the six-line hexaquo-Mn^{2+} EPR signal was measured (*55*, *56*). Whereas almost no hexaquo-Mn^{2+} EPR signal was observed during the initial period of illumination, a significant increase in the hexaquo-Mn^{2+} EPR signal was observed after prolonged illumination (Figure 2C).

$OH^{\bullet}$ Production in Mn-Depleted PSII. To test the involvement of the Mn-complex in the production of $OH^{\bullet}$, the time dependence of the formation of the POBN-OH adduct EPR signal was measured in hydroxylamine-treated PSII membranes. Mn-depletion results in a significant suppression of $OH^{\bullet}$ production (Figure 3A, trace b) compared to active PSII membranes (Figure 3A, trace a). The residual production of $OH^{\bullet}$ observed in Mn-depleted PSII membranes could be due to oxidizing reactions on the PSII donor side as proposed by Hideg et al. (*30*). The decrease in the production of $OH^{\bullet}$ might be a consequence of either the loss of the Mn-complex itself or the loss of electron donation from the Mn-complex to PSII. To test this, the time dependence of the POBN-OH adduct EPR signal was measured in Mn-depleted PSII membranes in the presence of an artificial donor, DPC, which donates electrons to $Tyr_z^{\bullet}$. In the presence of DPC, the light-induced production of $OH^{\bullet}$ was restored (Figure 3A, trace c). The same effect was observed when electron donation was supported by 1 mM NH_2OH (data not shown). Furthermore, the addition of 30 μM DCPIP to Mn-depleted PSII membranes in the presence of DPC completely diminish $OH^{\bullet}$ production (Figure 3A, trace d). Thus, it is evident that PSII electron-transfer reactions inside the PSII are essential for the production of $OH^{\bullet}$, whereas the Mn-complex itself is not required.

$OH^{\bullet}$ Production under Anaerobic Conditions. To study the effect of oxygen on the production of $OH^{\bullet}$, the time dependence of the light-induced production of $OH^{\bullet}$ was measured under anaerobic conditions (Figure 3B). The removal of oxygen by gentle flushing of PSII membranes with argon before illumination results in a significant inhibition of $OH^{\bullet}$ production (Figure 3B, trace b) compared to $OH^{\bullet}$ production measured in air (Figure 3B, trace a). To prevent the involvement of oxygen produced by PSII itself, $OH^{\bullet}$ production was measured in PSII membranes that were flushed with a gentle stream of argon during the illumination (Figure 3B, trace c). Under such conditions, only a residual production of $OH^{\bullet}$ was observed. On the other hand, increasing the oxygen concentration by flushing PSII membranes with oxygen results in an increase in $OH^{\bullet}$ production (Figure 3B, trace d). These observations indicate that oxygen is involved in the production of $OH^{\bullet}$.

Effect of SOD, Catalase and a Chelating Agent on $OH^{\bullet}$ Production. To study the involvement of $O_2^{\bullet-}$ and H_2O_2 in the production of $OH^{\bullet}$, the time dependence of $OH^{\bullet}$ production was measured in the presence of exogenous SOD and catalase (Figure 4A). Removal of $O_2^{\bullet-}$ by SOD results in the complete loss of $OH^{\bullet}$ production during the first phase, whereas it had no effect on the second phase (Figure 4A, trace b). On the other hand, the removal of H_2O_2 by the addition of catalase had no effect on the first phase; however, it did suppress the production of $OH^{\bullet}$ during the second phase

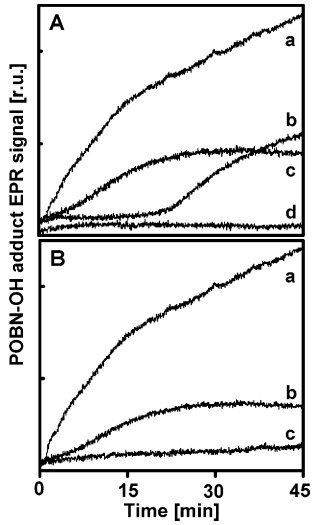

FIGURE 4: (A) Time dependence of the POBN-OH adduct EPR signal measured in the presence of (a) no additives, (b) SOD, (c) catalase, and (d) SOD + catalase. SOD (400 U mL^{-1}) and catalase (5000 U mL^{-1}) were added to PSII membranes before illumination. (B) Time dependence of POBN-OH adduct EPR signal measured in the presence of (a) no additives, (b) EDTA, and (c) SOD + EDTA. 1 mM EDTA was added to PSII membranes before illumination. EPR conditions as in Figure 3.

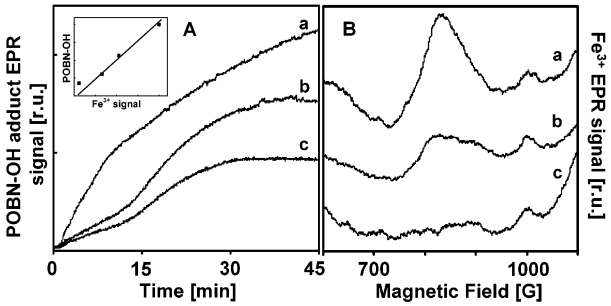

FIGURE 5: (A) Time dependence of the POBN-OH adduct EPR signal and (B) Fe^{3+} ($g = 8$) EPR signal in PSII membranes measured at (a) pH 6.5, (b) pH 5.5, and (c) pH 5. Inset shows the correlation between the POBN-OH adduct and the Fe^{3+} EPR signal at low pH. In (A) EPR conditions as in Figure 3. In (B), PSII membranes were incubated in the presence of 5 mM potassium ferricyanide for 30 min on ice in the dark. EPR conditions: temperature, 4.2 K; microwave power, 8 mW; modulation amplitude, 16 G; modulation frequency, 100 kHz; conversion time, 81.92 ms; time constant, 163.84 ms.

(Figure 4A, trace c). In the presence of both SOD and catalase (i.e., removal of both $O_2^{\bullet -}$ and H_2O_2), the production of OH• was almost completely abolished (Figure 4A, trace d).

To test the involvement of divalent metal ions in the production of OH•, the time dependence of OH• production was measured in the presence of a chelating agent, EDTA. The production of OH• during the first phase was insensitive to EDTA, whereas no OH• was observed during the second phase in the presence of EDTA (Figure 4B, trace b). In the presence of both SOD and EDTA, the production of OH• was almost completely prevented (Figure 4B, trace c). This observation shows that the presence of free divalent metal ions is essential for OH• production during the second phase, but not during the first phase.

Effect of Low pH on OH• Production. The time dependence of OH• production was measured at low pH (Figure 5A). When the pH decreases below 6.5, the POBN-OH adduct EPR signal was significantly suppressed during the first phase, while a small effect was observed during the second phase. At pH 5, only a residual POBN-OH adduct EPR signal was observed during the first phase (Figure 5A, trace c). Control experiments using the Fenton reagents, Fe^{2+} and H_2O_2, in the absence of PSII membranes showed no difference in the POBN-OH adduct EPR signal at pH 6.5 or at low pH, ruling out the possibility that the low pH effect was due to a pH dependence of the adduct (data not shown). These observations imply that OH• production is pH-dependent during the first phase, whereas OH• production during the second phase is rather pH insensitive.

The effect of low pH on the Fe^{3+} EPR signal at $g = 8$ generated by oxidation of the non-heme iron with potassium ferricyanide was measured. As is evident from Figure 5B, the pH decrease below 6.5 significantly diminished ferricyanide-induced Fe^{3+} EPR signal. At pH 5, almost no Fe^{3+} EPR signal was observed (Figure 5B, trace c). The decreased ability to oxidize non-heme iron using ferricyanide at low pH was previously demonstrated and assigned to an increase in the midpoint redox potential of Fe^{3+}/Fe^{2+} redox couple (*57*). When the amplitude of the POBN-OH adduct EPR signal measured after 7.5 min of illumination (i.e., $t_{1/2}$ of the first phase) was plotted against the amplitude of Fe^{3+} EPR signal, a linear correlation is observed (Figure 5A, inset). This correlation between POBN-OH adduct and Fe^{3+}/Fe^{2+} EPR signals could indicate that the Fe^{3+}/Fe^{2+} redox couple is involved in the formation of OH•.

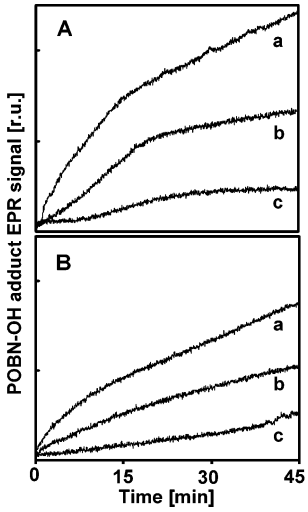

FIGURE 6: Time dependence of POBN-OH adduct EPR signal measured in (A) intact PSII membranes and (B) Mn-depleted PSII membranes plus DPC in the presence of (a) no additives, (b) 5 mM sodium formate, and (c) 100 mM sodium formate. Sodium formate was added to PSII membranes before illumination. EPR conditions as in Figure 3.

Effect of Formate on OH• Production. Formate is known to bind to the non-heme iron in PSII (*48*, *57*). We have observed that sodium formate decreases the production of OH• in intact and Mn-deleted PSII membranes in the presence of DPC (Figure 6). While formate can have effects on the donor and the acceptor side of PSII, this result is nevertheless consistent with the idea that the non-heme iron plays a role in OH• production.

Effect of Illumination on the EPR Signal from $Q_A^-Fe^{2+}$ and Fe^{3+}. The effect of illumination on the $Q_A^-Fe^{2+}$ and the Fe^{3+} EPR signals was measured. The $Q_A^-Fe^{2+}$ EPR

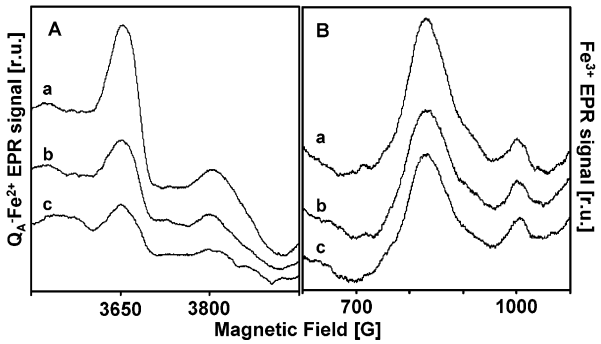

FIGURE 7: Effect of illumination on (A) the Q_A^- Fe^{2+} ($g = 1.84$) and (B) the Fe^{3+} ($g = 8$) EPR signal in PSII membranes illuminated for (a) 0, (b) 15, and (c) 45 min. After dark adaptation for 10 min, the sample was illuminated at 200 K for 10 min in the presence of 100 mM sodium formate (A) or incubated with 5 mM potassium ferricyanide for 30 min (B). The EPR conditions in (A) were microwave power; 32 mW; modulation amplitude, 32 G; the other conditions as in Figure 5B; in (B) as in Figure 5B.

signal at $g = 1.84$ induced by illumination of PSII membranes at 200 K in the presence of formate was found to decrease with illumination time (Figure 7A). Under our experimental conditions, the amplitude of the $Q_A^-Fe^{2+}$ EPR signal measured after 45 min of illumination decreases to about 50% of nonilluminated sample. This observation is in agreement with previous observations, which show a similar decrease in the $Q_A^-Fe^{2+}$ EPR signal (*58*, *59*).

The Fe^{3+} EPR signal at $g = 8$ generated by oxidation of non-heme iron with potassium ferricyanide was observed to decrease with illumination time (Figure 7B). Illumination for 45 min results in a drop in the amplitude of the Fe^{3+} EPR signal to 75% of that observed in nonilluminated sample. The decrease in the Fe^{3+} EPR signal implies that potassium ferricyanide is not able to oxidized non-heme Fe^{3+}. A light-induced decrease in the ability to oxide non-heme iron with ferricyanide was demonstrated previously and assigned to the redox changes of the non-heme iron (*59*, *60*).

DISCUSSION

Production of $OH^•$, $O_2^{•-}$, and H_2O_2 on the PSII Acceptor Side. The results presented in this study show that high light intensity illumination of spinach PSII membranes results in the generation of $OH^•$ (Figure 1A). It has been previously proposed that $OH^•$ is produced on the PSII acceptor side via Fenton chemistry (*12*, *27*). Here we show that the depletion of Mn-complex results in the suppression of $OH^•$ production, whereas the addition of an artificial electron donor DPC to Mn-depleted PSII membranes restores the production of $OH^•$ (Figure 3A). This observation and our previous result that addition of an artificial electron acceptor, DCPIP, brings about the suppression of $OH^•$ production in both active (*21*) and Mn-depleted PSII membranes (Figure 3A, trace d) indicate that $OH^•$ is produced on the PSII acceptor side. This proposal is in line with the observation that the production of $OH^•$ is dependent on the presence of oxygen (Figure 3B) and that removal of all oxygen and H_2O_2 by glucose/glucose oxidase/catalase enzyme system decreases significantly the production of $OH^•$ in PSII membranes (*27*). The requirement of oxygen for the production of $OH^•$ shows that molecular oxygen is involved in the reaction pathway of $OH^•$ production on the PSII acceptor side.

In addition to $OH^•$, illumination of PSII membranes results in the formation of $O_2^{•-}$ (Figure 1B). In accordance with this observation, it has been demonstrated using the DEPMPO spin-trap compound, that illumination of PSII membranes gives rise to the production of both $O_2^{•-}$ and $OH^•$ (*12*, *13*). It has been proposed that $O_2^{•-}$ is formed by reduction of molecular oxygen on the PSII acceptor side (*10*, *11*, *21*) and that dismutation of $O_2^{•-}$ results in the formation of H_2O_2 (*10*, *17*, *22*). In the accordance with Schröder and Åkerlund (*22*), we demonstrated that production of H_2O_2 is dependent on the presence of oxygen (Figure 2A, trace b), indicating that under our experimental conditions reduction of molecular oxygen is likely involved in the H_2O_2 production.

Given the limited electron acceptor capacity of PSII membranes, it seems likely that the limited quinone pool (including any functional Q_B) will be fully reduced and that Q_A will be trapped as its semiquinone form after a small number of turnovers. Under these conditions, charge separation to form $P680^+Pheo^-$ occurs only at a relatively low quantum yield. The reduction of O_2 forming superoxide is the main forward electron-transfer reaction. It is unclear which reduced electron acceptor is the actual donor to O_2 however the most likely candidates are the Q_A^-, the only quinone in the reactive semiquinone state, or the shorter lived but more reducing $Pheo^-$. It is possible that the dominant reductant of O_2 changes over the course of the reaction, being Q_A^- in the early phase and the $Pheo^-$ at later times. Future experiments could clarify this question.

Involvement of the PSII Electron Donor Side in the Generation of $OH^•$, $O_2^{•-}$, and H_2O_2. In this work, we have found no indication that the electron donor side of PSII is involved in the formation of the reactive oxygen species. In the literature, there are several reports to the contrary. However, we consider that there is no real contradiction since the experimental conditions used here would be expected to minimize any donor side involvement and as such are quite distinct from those used in the earlier reports.

The formation of H_2O_2 on the PSII electron donor side is expected only under specific inhibitory conditions such as depletion of 17, 23, and/or 33 kDa extrinsic proteins (*17*, *18*, *61*) or chloride (*19*, *20*). The generation of $OH^•$ and $O_2^{•-}$ with donor side involvement was reported in Mn-depleted in the absence of an efficient electron donor (*14*, *15*, *30*). It was suggested that long-lived oxidizing species such as $P680^+$ or $Tyr_z^•$ were involved in generating both $OH^•$ and $O_2^{•-}$. In the present work, such processes would have been minimized since we used either intact PSII or Mn-depleted PSII plus an efficient electron donor. We do not rule out however that after long periods of illumination, when the centers are damaged to different degrees, that electron donor side reactions could potentially contribute to the formation of activated oxygen species to a small extent.

$O_2^{•-}$ and H_2O_2 as Intermediates in $OH^•$ Production. The question arises whether $O_2^{•-}$ and H_2O_2 are intermediates in the production of $OH^•$ on the PSII acceptor side. The observation that during the first phase the dismutation of $O_2^{•-}$ with SOD inhibited production of $OH^•$ (Figure 4A, trace b) indicates that $O_2^{•-}$ is involved in the production of $OH^•$, but it is unlikely that the reaction pathway involves free H_2O_2. This suggestion is supported by the observation that scavenging of free H_2O_2 with catalase brings about no effect on

the production of OH• during the first phase (Figure 4A, trace c). The explanation for these observations is that OH• is produced either directly from $O_2^{\bullet-}$, bypassing dismutation to H_2O_2, or indirectly via reduction of $O_2^{\bullet-}$ forming a bound peroxide that is insensitive to catalase. As for thermodynamic reasons the direct reduction of $O_2^{\bullet-}$ to OH• is unfavorable, the formation of bound peroxide is the more likely explanation.

On the other hand, the observation that during the second phase the production of OH• is unaffected by the dismutation of $O_2^{\bullet-}$ (Figure 4A, trace b) implies that OH• likely originates from $O_2^{\bullet-}$ via a reaction pathway involving free H_2O_2. The observation that production of OH• during the second phase is significantly diminished by scavenging the free H_2O_2 (Figure 4A, trace c) confirms that OH• originates from free H_2O_2. Taking these observations together, it is reasonable to suggest that OH• detected during the first phase is produced by the reduction of bound peroxide, which is probably formed by the interaction of $O_2^{\bullet-}$ with a metal center in PSII, whereas OH• generated during the second phase is produced from free H_2O_2 formed by dismutation of $O_2^{\bullet-}$.

The two different origins of hydroxyl radicals might also be related to the two phases of loss of oxygen evolving activity shown in Figure 2B. When OH• is formed from bound peroxide, the probability of a damaging reaction of OH• with the acceptor side of PSII is more likely compared with the situation of OH• formed from free peroxide. OH• has a very short lifetime, and, due to the diffusion time and distance necessary to react with PSII, the inhibitory potential of OH• might be expected to be lower during the second phase of photoinhibitory illumination.

Formation and Reduction of Peroxide at the PSII Metal Center. Three metal centers are potential candidates for the site of bound peroxide: the Mn-complex, cyt b_{559}, and the non-heme iron. Because of the observation that the Mn-complex itself is not required for the formation of OH• (Figure 3A), the involvement of the Mn-complex in the binding and reduction of peroxide can be excluded. Furthermore, the non-heme iron has exchangeable ligands under normal functional conditions, while this has not been demonstrated for the cytochrome heme. Furthermore, it is well known that formate can bind to the non-heme iron (for example ref *48*), and indeed we found here that formate inhibits OH• formation in intact and Mn-depleted PSII. These arguments and results then make the non-heme iron the more likely candidate. Redox arguments support this viewpoint.

As the midpoint redox potential of the OH•/H_2O_2 redox couple is 460 mV (pH 7) (*62*), either the heme iron of cyt b_{559} (high potential form 400 mV) or the non-heme iron (400 mV) might reduce H_2O_2 to OH•. However, several forms of Cyt b_{559} have been reported: high-potential (HP) cyt b_{559} (400 mV), intermediate-potential (IP) cyt b_{559} (200 ± 50 mV), and low-potential (LP) cyt b_{559} (60 ± 50 mV) (*63*). The removal of the Mn is known to shift heme to its lower potential forms, and yet the phase of OH• attributed to the bound peroxide route is unaffected upon Mn removal. This might be taken as arguing against a role for the heme in the bound peroxide route for OH• formation.

The redox potential of HP cyt b_{559} was shown to be pH insensitive, whereas the redox potential of LP Cyt b_{559} increases by 60 mV per unit at low pH (*64*−*66*). The midpoint redox potential of the non-heme iron is 400 mV (pH 7) and increases by 60 mV per unit at low pH (*57*). Our results presented in Figure 5A demonstrate that the production of OH• during the first phase was prevented at low pH. One possible explanation for this observation is that a pH decrease brings about an increase in the midpoint redox potential of the non-heme iron above 460 mV and makes the reduction of H_2O_2 to OH• less favorable. This argument however is weakened by the fact that superoxide spontaneously dismutates more rapidly at low pH (see below), and this might contribute to the effects seen in Figure 5A.

Overall, based on these considerations, it is suggested that the non-heme iron is the most likely candidate as the site for bound peroxide formation and its reduction to OH•. In accordance with this proposal, it has been demonstrated that incubation of PSII membranes with glucose-glucose oxidase in the aerobic conditions induces a significant oxidation of the non-heme iron, probably due to formation of H_2O_2 (*49*, *57*). Furthermore, H_2O_2 treatment of PSII core complexes, which contain the non-heme iron, was shown to cause more pronounced damage to the proteins than when isolated PSII reaction centers, which lack the non-heme iron, are treated with H_2O_2 (*58*, *67*). Because of the observation that a residual level of H_2O_2 disproportion was observed in catalase-free PSII membranes, it was suggested that the non-heme iron might reduce H_2O_2 via Fenton chemistry (*28*). However, the involvement of heme iron of cyt b_{559} in the reduction of peroxide to OH• cannot be ruled out. The fraction of LP cyt b_{559} was shown to be transiently oxidized by H_2O_2 in the presence of excess ascorbate (*69*).

Dismutation of $O_2^{\bullet-}$ and Fenton Chemistry in PSII. Apart from the interaction of $O_2^{\bullet-}$ with PSII metal center and the formation of the iron-peroxide complex, it is suggested that a fraction of $O_2^{\bullet-}$ dismutates to form free H_2O_2 (Figure 2A). In the presence of exogenous SOD, the dismutation of $O_2^{\bullet-}$ to free H_2O_2 is stimulated and thus the formation of OH• via a bound peroxide intermediate is prevented (Figure 4A, trace b). A similar effect was observed at low pH (Figure 5A, traces b and c). It is well established that the anionic form of $O_2^{\bullet-}$ is in pH-dependent equilibrium with its protonated form perhydroxyl radical ($HO_2^{\bullet}$), which has a pK of approximately 4.8 (*8*, *70*). As $HO_2^{\bullet}$ dismutates spontaneously to free H_2O_2 by several orders of magnitude faster than does $O_2^{\bullet-}$, the spontaneous dismutation of $O_2^{\bullet-}$ to free H_2O_2 is significantly stimulated at low pH and thus the production of OH• via an iron-peroxide intermediate is diminished.

On the basis of the observation that the production of OH• during the second phase requires free divalent metals (Figure 4B), it is proposed that free divalent metals mediate the reduction of free H_2O_2 to OH•. Even if free H_2O_2 is produced during the whole period of illumination (Figure 2A), due to the lack of free divalent ions during the first phase, free H_2O_2 is not reduced to OH•. It is suggested that free H_2O_2 is gradually accumulated in the medium, and this reduces the Mn-complex causing its disassembly and release of Mn^{2+} (Figure 2C) (see for example ref *71*). It is suggested that Mn^{2+} might be involved in the reduction of H_2O_2 to OH•. This suggestion is supported by the observation that no production of OH• was observed in the presence of endogenous SOD and EDTA (Figure 4B, trace c). Under such conditions, all $O_2^{\bullet-}$ dismutates to free H_2O_2; however, due

Scheme 2[a]

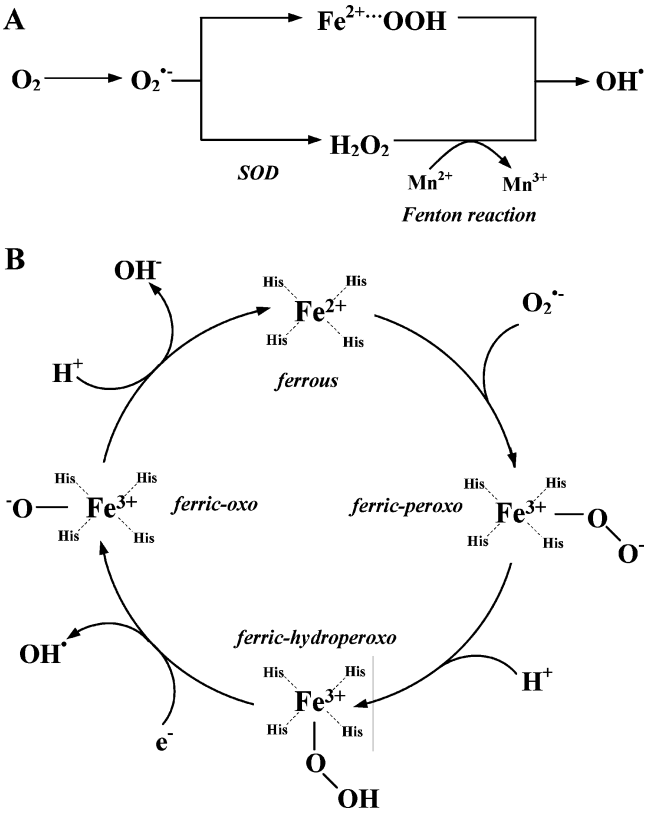

[a] (A) Bound peroxide (upper route) and free peroxide (lower route) reaction pathways for the production of $OH^{\bullet}$ on the PSII acceptor side. (B) Proposed model for the involvement of iron-peroxo intermediates in $OH^{\bullet}$ production.

to the chelating of divalent ions H_2O_2 was not reduced to $OH^{\bullet}$.

Two-Site Model of $OH^{\bullet}$ Production. On the basis of the results presented here, a model for $OH^{\bullet}$ production in PSII membranes is proposed (Scheme 2A). Two reaction pathways are suggested to be involved in the production of $OH^{\bullet}$ on the PSII acceptor side: (1) the bound peroxide pathway and (2) the free peroxide pathway. In the former reaction pathway, the reduction of peroxide bound to the PSII metal center is assumed to result in the formation of $OH^{\bullet}$. The source of electrons for this reduction process is proposed to come from photosynthetic charge separation. In the free peroxide reaction pathway, $OH^{\bullet}$ is suggested to be formed by the reduction of free H_2O_2 via the Fenton reaction.

(1) Bound Peroxide Pathway. In the proposed model, the non-heme iron is assumed to be the site of the formation of iron-peroxo intermediates in the bound peroxide pathway for $OH^{\bullet}$ production (Scheme 2B). The interaction of $O_2^{\bullet-}$ and the non-heme iron is suggested to result in rapid oxidation of the ferrous Fe^{2+} and the formation of a ferric-peroxo species. It is postulated that the transfer of an electron from Fe^{2+} to a coordinated $O_2^{\bullet-}$ occurs as an inner-sphere electron-transfer reaction. The ferric-peroxo species is proposed to be protonated to form a ferric-hydroperoxo species. The mechanism for formation of the ferric-hydroperoxo species is proposed based on the analogy with superoxide reductase (SOR) (*44*, *72*). SOR is an enzyme containing a non-heme iron that catalyzes only one of the two reactions of SOD, i.e., the reduction of $O_2^{\bullet-}$ to H_2O_2. The non-heme iron in SOR is liganded by four histidines and a cystein [$Fe(His)_4$-(Cys)] (*73*, *74*), similar to the four histidines and bicarbonate that make up the ligand sphere of non-heme iron in PSII. In SOR, the cystein can be replaced by CN^- (*75*) or NO (*76*), while these exogenous ligands can replace the bicarbonate in PSII (*77*, *78*). In the second part of the reaction cycle, the reduction of the ferric-hydroperoxo species is suggested to result in the formation of $OH^{\bullet}$. In this reaction, the ferric iron is proposed to be reduced by an endogenous reductant, the most likely being Q_A^-, whereas the ferrous iron produced is suggested to reduce the hydroperoxo ligand. The reduction is believed to occur as an inner-sphere electron-transfer reaction and to yield a ferric-oxo intermediate (*33*, *36*, *37*).

(2) Free Peroxide Pathway. The dismutation of $O_2^{\bullet-}$ is proposed to result in the production of free H_2O_2 (*17*, *10*, *22*). It is suggested that $O_2^{\bullet-}$ dismutates either spontaneously or is catalyzed by an intrinsic SOD. It has been suggested that the cyt b_{559} may play this role (*10*, *23*). Free Mn^{2+} or other metal ions are suggested to reduce free H_2O_2 to $OH^{\bullet}$.

Relevance to Physiological Oxidative Stress in PSII. The presented data were obtained with isolated PSII membranes without an added electron acceptor. While these are obviously not physiological conditions, the two reaction pathways for production of $OH^{\bullet}$, which are proposed here, may have relevance under certain physiological conditions although occurring at lower yields. Because of its early occurrence, it is possible that the generation of $OH^{\bullet}$ via the bound peroxide pathway, a process that by its nature occurs within the reaction center, contributes significantly to photodamage, particularly the impairment of the semiquinone−iron complex (Figure 7). The mechanism put forward here involving the binding of superoxide by a PSII metal center, forming a bound peroxide intermediate, is therefore worth considering as a relevant reaction in photoinhibiton of PSII under physiological conditions.

ACKNOWLEDGMENT

The authors thank Charilaos Goussias and Tony Mattioli for stimulating discussion.

REFERENCES

1. Nugent, J. H. A. (1996) Oxygenic photosynthesis. Electron transfer in photosystem I and photosystem II, *Eur. J. Biochem. 237*, 519−531.
2. Britt, R. D. (1996) Oxygen Evolution, in *Oxygenic Photosynthesis: The Light Reactions* (Ort, D., Yocum, C., Eds.) pp 137−164, Kluwer Academic Publishers, Dordrecht, The Netherlands.
3. Diner, B. A., and Babcock, G. T. (1996) Structure, Dynamics, and Energy Conversion Efficiency in Photosystem II, in *Oxygenic Photosynthesis: The Light Reactions* (Ort, D., Yocum, C., Eds.) pp 213−247, Kluwer Academic Publishers, Dordrecht, The Netherlands.
4. Diner, B. A., and Rappaport, F. (2002) Structure, dynamics, and energetics of the primary photochemistry of photosystem II of oxygenic photosynthesis, *Annu. Rev. Plant. Biol. 53*, 551−580.
5. Goussias, C., Boussac, A., Rutherford, A. W. (2002) Photosystem II and photosynthetic oxidation of water: an overview, *Philos. Trans. R. Soc. London B. 357*, 1369−1381.
6. Foyer, C. (1997) Oxygen Metabolism and Electron Transport in Photosynthesis, in *Oxidative Stress and the Molecular Biology of Antioxidant Defences* (Scandalios, J. G., Ed.) pp 587−621, Cold Spring Harbor Laboratory Press, Plainview, NY.
7. Elstner, E. F. (1982) Oxygen activation and oxygen toxicity, *Annu. Rev. Plant. Physiol. 33*, 73−96.
8. Halliwell, B., and Gutteridge, J. M. (1999) in *Free Radicals in Biology and Medicine*, 3rd ed., Oxford University Press, New York.

9. Asada, K. (1999) The water−water cycle in chloroplasts: scavenging of active oxygens and dissipation of excess photons, *Annu. Rev. Plant. Physiol. Plant. Mol. Biol. 50*, 601−639.
10. Ananyev, G. M., Renger, G., Wacker, U., and Klimov, V. V. (1994) The production of superoxide radicals and the superoxide dismutase activity of photosystem II. The possible involvement of cytochrome b_{559}, *Photosynth. Res. 41*, 327−338.
11. Cleland, R. E., and Grace, S. C. (1999) Voltammetric detection of superoxide production by photosystem II, *FEBS Lett. 457*, 348−352.
12. Navari-Izzo, F., Pinzino, C., Quartacci, M. F., and Sgherri, C. L. M. (1999) Superoxide and hydroxyl radical generation, and superoxide dismutase in PSII membrane fragments from wheat, *Free Radical Res. 30*, 3−9.
13. Zhang, S., Weng, J., Pan, J., Tu, T., Yao, S., and Xu, C. (2003) Study on the photogeneration of superoxide radicals in Photosystem II with EPR spin trapping techniques, *Photosynth. Res. 75*, 41−48.
14. Chen, G. X., Blubaugh, D. J., Homann, P. H., Golbeck, J. G., and Cheniae, G. M. (1995) Superoxide contributes to the rapid inactivation of specific secondary donors of the photosystem II reaction center during photodamage of manganese-depleted photosystem II membranes, *Biochemistry 34*, 2317−2332.
15. Chen, G. X., Kazimir, J., and Cheniae, G. M. (1992) Photoinhibition of hydroxylamine-extracted photosystem II membranes: studies of the mechanism, *Biochemistry 31*, 11072−11083.
16. Schröder, W. P., and Åkerlund, H.-E. (1986) H_2O_2 accessibility to the Photosystem II donor side in protein-depleted inside-out thylakoids measured as flash-induced oxygen production, *Biochim. Biophys. Acta 848*, 359−363.
17. Klimov, V., Ananyev, G., Zastryzhnava, O., Wydrzynski, T., and Renger, G. (1993) Photoproduction of hydrogen peroxide in photosystem II membrane fragments: a comparison of four signals, *Photosynth. Res. 38*, 409−416.
18. Hillier, W., and Wydrzynski, T. (1993) Increases in peroxide formation by the Photosystem II oxygen evolving reactions upon removal of the extrinsic 16, 22 and 33 kDa proteins are reversed by $CaCl_2$ addition, *Photosynth. Res. 38*, 417−423.
19. Fine, P. L., and Frasch, W. D. (1992) The oxygen-evolving complex requires chloride to prevent hydrogen peroxide formation, *Biochemistry 31*, 12204−12210.
20. Krieger, A., and Rutherford, A. W. (1998) The Involvement of H_2O_2 Produced by Photosystem II in Photoinhibition, in *Photosynthesis: Mechanisms and Effects* (Garab, G., Ed.) Vol. 3, pp 2135−2138, Kluwer Academic Publishers, Dordrecht, The Netherlands.
21. Arató, A., Bondarava, N., and Krieger-Liszkay, A. (2004) Production of reactive oxygen species in chloride- and calcium depleted photosystem II and their involvement in photoinhibition, *Biochim. Biophys. Acta 1608*, 171−180.
22. Schröder, W. P., and Åkerlund, H.-E. (1990) Hydrogen Peroxide Production in Photosystem II Preparations, in *Current Research in Photosynthesis* (Baltscheffsky, M., Ed.) Vol. 1, pp 901−904, Kluwer Academic Publisher, Dordrecht, The Netherlands.
23. Kruk, J., and Strzalka, K. (1999) Dark reoxidation of the plastoquinone-pool is mediated by the low-potential form of cytochrome b_{559} in spinach thylakoids, *Photosynth. Res. 62*, 273−279.
24. Nugent, J. H. A. (2001) Photoreducible high spin iron electron paramagnetic resonance signals in dark-adapted Photosystem II: are they oxidised nonhaem iron formed from interaction of oxygen with PSII electron acceptors? *Biochim. Biophys. Acta 1504*, 288−298.
25. Wydrzynski, T., Huggins, B. J., and Jursinic, P. A. (1985) Uncoupling of detectable O_2 evolution from the apparent S-state transitions in Photosystem II by lauroylcholine chloride: possible implicationsin the photosynthetic water-splitting mechanism, *Biochim. Biophys. Acta 809*, 125−136.
26. Wydrzynski, T., Hillier, W., and Messinger, J. (1996) On the functional significance of substrate accessibility in the photosynthetic water oxidation mechanism, *Physiol. Plant. 96*, 342−350.
27. Yruela, I., Pueyo, J. J., Alonso, P. J., and Picorel, R. (1996) Photoinhibition of photosystem II from higher plants. Effect of copper inhibition, *J. Biol. Chem. 271(44)*, 27408−27415.
28. Sheptovitsky, Y. G., and Brudvig, G. W. (1998) Catalase-free photosystem II: the O_2-evolving complex does not dismutate hydrogen peroxide, *Biochemistry 37*, 5052−5059.
29. Fufezan, C., Rutherford, A. W., and Krieger-Liszkay, A. (2002) Singlet oxygen production in herbicide-treated photosystem II, *FEBS Lett. 532*, 407−410.
30. Hideg, É., Spetea, C., and Vass, I. (1994) Singlet oxygen and free radical production during acceptor- and donor-side-induced photoinhibition. Studies with spin trapping EPR spectroscopy, *Biochim. Biophys. Acta 1186*, 143−152.
31. Zolla, L., and Rinalducci, S. (2002) Involvement of active oxygen species in degradation of light-harvesting proteins under light stresses, *Biochemistry 41*, 14391−14402.
32. Liochev, S. I. (1999) The Mechanism of "Fenton-Like" Reactions and Their Importance for Biological Systems. A Biologist's View, in *Metals in Biological Systems* (Sigel, A., Sigel, H., Eds.) Vol. 36, pp 1−39, Marcel Dekker, Inc, New York.
33. Branchaud, B. P. (1999) Free Radicals as a Results of Dioxygen Metabolism, in *Metals in Biological Systems* (Sigel, A., Sigel, H., Eds.) Vol. 36, pp 79−102, Marcel Dekker, Inc, New York.
34. Elstner, E. F., Osswald, W., and Konze, J. R. (1980) Reactive oxygen species: electron donor-hydrogen peroxide complex instead of free radicals? *FEBS Lett. 121*, 219−221.
35. Stadtman, E. R. (1993) Oxidation of free amino acids and amino acid residues in proteins by radiolysis and by metal-catalyzed reactions, *Annu. Rev. Biochem. 62*, 797−821.
36. Sawyer, D. T., Kang, C., Llobet, A., and Redman, C. (1993) Fenton reagents (1:1 Fe^{II} L_x/HOOH) react via [$L_xFe^{II}OOH(BH^+)$] (1) as hydroxylases (RH−ROH), not as generators of free hydroxyl radicals (HO•), *J. Am. Chem. Soc. 115*, 5817−5818.
37. Sawyer, D. T., Sobkowiak, A., and Matsushita, T. (1996) Metal [ML_x; M = Fe, Cu, Co, Mn]/hydroperoxide-induced activation of dioxygen for the oxygenation of hydrocarbons: oxygenated Fenton chemistry, *Acc. Chem. Res. 29*, 409−416.
38. Fridovich, I. (1998) Oxygen toxicity: a radical explanation, *J. Exp. Biol. 201*, 1203−1209.
39. Sono, M., Roach, M. P., Coulter, E. D., and Dawson, J. H. (1996) Heme-containing oxygenases, *Chem. Rev. 96*, 2841−2887.
40. Burger, R. M. (2000) Nature of activated bleomycin, *Struct. Bonding 97*, 287−303.
41. Ortiz de Montellano, P. R. (1998) Heme oxygenase mechanism: evidences for an electrophilic, ferric peroxide species, *Acc. Chem. Res. 31*, 543−549.
42. Jenney, F. E., Jr., Verhagen, M. F. J. M., Cui, X., and Adams, M. W. W. (1999) Anaerobic microbes: oxygen detoxification without superoxide dismutase, *Science 286*, 306−309.
43. Coulter, E. D., Emerson, J. P., Kurtz, D. M., Jr., and Cabelli, D. E. (2000) Superoxide reactivity of rubredoxin oxidoreductase (desulfoferrodoxin) from *Desulfovibrio vulgaris*: a pulse radiolysis study, *J. Am. Chem. Soc. 122*, 11555−11556.
44. Mathé, C., Mattioli, T. A., Horner, O., Lombard, M., Latour, J.-M., Fontecave, M., and Nivière, V. (2002) Identification of iron(III) peroxo species in the active site of the superoxide reductase SOR from Desulfoarculus baarsii, *J. Am. Chem. Soc. 124*, 4966−4967.
45. Berthold, D. A., Babcock, G. T., and Yocum, C. F. (1980) A highly resolved, oxygen evolving photosystem II preparation from spinach thylakoid membranes, *FEBS Lett. 134*, 231−234.
46. Ford, R. C., and Evans, M. C. W. (1983) Isolation of a photosystem 2 preparation from higher plants with highly enriched oxygen evolution activity, *FEBS Lett. 160*, 159−164.
47. Rutherford, A. W., and Zimmermann, J. L. (1984) A new EPR signal attributed to the primary plastoquinone acceptor in Photosystem II, *Biochim. Biophys. Acta 767*, 168−175.
48. Vermass, W. F. J., and Rutherford, A. W. (1984) EPR measurements on the effect of bicarbonate and triazine resistance in the acceptor side of Photosystem II, *FEBS Lett. 175*, 243−248.
49. Petrouleas, V., and Diner, B. A. (1986) Identification of Q_{400}, a high-potential electron acceptor of Photosystem II, with the iron of the quinone-iron complex, *Biochim. Biophys. Acta 849*, 264−275.
50. Janzen, E. G., Kotake, Y., and Hinton, R. D. (1992) Stabilities of hydroxyl radical spin adducts of PBN-type spin traps, *Free Radical Biol. Med. 12*, 169−173.
51. Pou, S., Ramos, C. L., Gladwell, T., Renks, E., Centra, M., Young, D., Cohen, M. S., and Rosen, G. M. (1994) A kinetic approach to the selection of a sensitive spin trapping system for the detection of hydroxyl radical, *Anal. Biochem. 217*, 76−83.
52. Olive, G., Mercier, A., Moigne, F. L., Rockenbauer, A., Tordo, P. (2000) 2-ethoxycarbonyl-2-methyl-3,4-dihydro-2H-pyrrole-1-oxide: evaluation of the spin trapping properties, *Free Radical Biol. Med. 28*, 403−408.

53. Zhang, H., Joseph, J., Vasquez-Vivar, J., Karoui, H., Nsanzumuhire, C., Martasek, P., Tordo, P., and Kalyanaraman, B. (2000) Detection of superoxide anion using an isotopically labeled nitrone spin trap: potential biological applications, *FEBS Lett. 473*, 58−62.
54. Kirilovsky, D., and Etienne, A.-L. (1991) Protection of reaction center II from photodamage by low temperature and anaerobiosis in spinach chloroplasts, *FEBS Lett. 279*, 201−204.
55. Yocum, C. F., Yerkes, C. T., Blankenship, R. E., Sharp, R. R., and Babcock, G. T. (1981) Stoichiometry, inhibitor sensitivity, and organization of manganese associated with photosynthetic oxygen evolution, *Proc. Natl. Acad. Sci. U.S.A. 78*, 7507−7511.
56. Sandusky, P. O., and Yocum, C. F. (1988) Hydrogen peroxide oxidation catalyzed by chloride-depleted thylakoid membranes, *Biochim. Biophys. Acta 936*, 149−156.
57. Petrouleas, V., and Diner, B. A. (1987) Light-induced oxidation of the acceptor-side Fe(II) of Photosystem II by exogenous quinones acting throught the Q_B binding site. I. Quinones, kinetics and pH-dependence, *Biochim. Biophys. Acta 893*, 126−137.
58. Styring, S., Virgin, I., Ehrenberg, A., and Andersson, B. (1990) Strong light photoinhibition of electrotransport in Photosystem II. Impairment of the function of the first quinone acceptor, Q_A, *Biochim. Biophys. Acta 1015*, 269−278.
59. Vass, I., Sanakis, Y., Spetea, C., and Petrouleas, V. (1995) Effects of photoinhibition on the Q_A-Fe^{2+} complex of photosystem II studied by EPR and Mössbauer spectroscopy, *Biochemistry 34*, 4434−4440.
60. Gleiter, H. M., Nugent, J. H. A., Haag, E., and Renger, G. (1992) Photoinhibition affects the non-heme iron center in photosystem II, *FEBS Lett. 313*, 75−79.
61. Ananyev, G. M., Wydrzynski, T., Renger, G., and Klimov, V. V. (1992) Transient peroxide formation by the manganese-containing, redox-active donor side of Photosystem II upon inhibition of O_2 evolution with lauroylcholine chloride, *Biochim. Biophys. Acta 1100*, 303−311.
62. Pierre, J. L., and Fontecave, M. (1999) Iron and activated oxygen species in biology: the basic chemistry, *Biometals 12*, 195−199.
63. Whitmarsh, J., and Pakrasi, H. (1996) Form and Function on Cytochrome b_{559}, in *Oxygenic Photosynthesis: The Light Reactions* (Ort, D. R., Yocum, C. F., Eds.) Vol. 4, pp 249−264, Kluwer Academic Publishers, Dordrecht, The Netherlands.
64. Ortega, J. M., Hervas, M., and Losada, M. (1988) Redox and acid−base characterization of cytochrome b_{559} in photosystem II particles, *Eur. J. Biochem. 171*, 449−455.
65. Kaminskaya, O., Kurreck, J., Irrang, K.-D., Renger, G., and Shuvalov, V. (1999) Redox and spectral properties of cytochrome b_{559} in different preparations of photosystem II, *Biochemistry 35*, 16223−16235.
66. Roncel, M., Ortega, J. M., and Losada, M. (2001) Factors determining the special redox properties of photosynthetic cytochrome b_{559}, *Eur. J. Biochem. 268*, 4961−4968.
67. Satoh, K. (1992) Structure and Function of Photosystem II Reaction Center, in *Research in Photosynthesis* (Murata, N., Ed.) Vol. 2, pp 3−12, Kluwer Academic Publisher, Dordrecht, The Netherlands.
68. Miyao, M., Ikeuchi, M., Yamamoto, N., and Ono, T. (1995) Specific degradation of the D1 protein of photosystem II by treatment with hydrogen peroxide in darkness: implications for the mechanism of degradation of the D1 protein under illumination, *Biochemistry 34*, 10019−10026.
69. Heimann, S., and Schreiber, U. (1996) Characterisation of a H_2O_2-oxidisable cytochrome b_{559} in intact chloroplasts with a new type of LED Array Spectrophotometer, *Photosynth. Res. 47*, 187−197.
70. Bensasson, R. V., Land, E. J., and Truscott, T. G. (1993) Activated Forms of Oxygen, in *Excited State and Free Radicals in Biology and Medicine*, Oxford Science Publication, Oxford.
71. Thompson, L. K., Blaylock, R., Sturtevant, J. M., and Brudvig, G. W. (1989) Molecular basis of the heat denaturation of photosystem II, *Biochemistry 28*, 6686−6695.
72. Adams, M. W. W., Jenney, F. E., Jr., Clay, M. D., and Johnson, M. K. (2002) Superoxide reductase: fact or fiction? *J. Biol. Inorg. Chem. 7*, 647−652.
73. Yeh, A. P., Hu, Y., Jenney, F. E., Jr., Adams, M. W. W., and Rees, D. C. (2000) Structures of the superoxide reductase from Pyrococcus furiosus in the oxidized and reduced states, *Biochemistry 39*, 2499−2508.
74. Clay, M. D., Jenney, F. E., Jr., Hagedoorn, P. L., George, G. N., Adams, M. W. W., and Johnson, M. K. (2002) Spectroscopic studies of *Pyrococcus furiosus* superoxide reductase: implications for active-site structures and the catalytic mechanism, *J. Am. Chem. Soc. 124*, 788−805.
75. Shearer, J., Fitch, S. B., Kaminsky, W., Benedict, J., Scarrow, R. C., and Kovacs, J. A. (2003) How does cyanide inhibit superoxide reductase? Insight from synthetic $Fe^{III}N_4S$ model complexes, *Proc. Natl. Acad. Sci. U.S.A. 100(7)*, 3671−3676.
76. Clay, M. D., Cosper, C. A., Jenney, F. E., Jr., Adams, M. W. W., Johnson, M. K. (2003) Nitric oxide binding at the mononuclear active site of reduced *Pyrococcus furiosus* superoxide reductase, *Proc. Natl. Acad. Sci. U.S.A. 100*, 3796−3801.
77. Petrouleas, V., and Diner, B. A. (1990) Formation by NO of nitrosyl adducts of redox components of the Photosystem II reaction center. I. NO binds to the acceptor-side non-heme iron, *Biochim. Biophys. Acta 1015*, 131−140.
78. Koulougliotis, D., Kostoupoulos, T., Petrouleas, V., and Diner, B. (1993) Evidence for CN^- binding at the PSII non-heme Fe^{2+}. Effect on the EPR signal for $Q_A^-Fe^{2+}$ and Q_A/Q_B electron transfer, *Biochim. Biophys. Acta 1141*, 275−282.

BI036219I